

**Long-wavelength electromagnetic waves of surface type in circular metal waveguides partially filled by plasma in presence of an axial static magnetic field**

Igor O. Girka<sup>1,2</sup>, Manfred Thumm<sup>3</sup>

1 - V.N.Karazin Kharkiv National University, Svobody sq., 4, 61022, Kharkiv, Ukraine. (e-mail: igorgirka@karazin.ua).

2 – Max-Planck-Institut für Plasmaphysik, Boltzmannstrasse 2, 85748, Garching, Germany

3 – Karlsruhe Institute of Technology, IHM and IHE, 76131, Karlsruhe, Germany

**Abstract** – The method of successive approximations is applied to solve the Maxwell equations in cylindrical plasma waveguide geometry for electromagnetic waves with arbitrary azimuthal wave index and small axial wavenumber. The theory of surface flute waves is used as zeroth approximation. The study generalizes previous investigations whose results are utilized for the verification of newly obtained conclusions. The influences of several plasma waveguide parameters as magnitude and sign of the azimuthal wave index, the width of the dielectric layer between plasma and waveguide wall and the magnitude of its dielectric constant, the radii of the plasma column and the metal wall, and the external axial static magnetic field on the wave dispersion properties are analyzed.

**Keywords:** Long-wavelength electromagnetic surface waves, circular plasma waveguides, method of successive approximations, small axial wavenumber, axial static magnetic field, dispersion properties, group velocity

**I. Introduction**

Studying electromagnetic flute waves with zero axial wavenumber ( $k_z = 0$ ), can be of interest in different fields of plasma physics. A comprehensive overview of surface wave applications in the fields of plasma electronics, plasma-antenna systems, description of phenomena in the plasma periphery of magnetic confinement fusion devices, nano-technologies, and for plasma production is given in [1]. In

particular, surface flute waves can be of interest for plasma electronics due to their efficient interaction with an annular electron beam, which gyrates along large Larmor orbits around the plasma column [2-9].

Studying flute waves has the advantage that they are electromagnetic waves of ordinary (with the components  $E_z$ ,  $H_r$ , and  $H_\phi$  of the wave fields) and extraordinary (with the components  $H_z$ ,  $E_r$ , and  $E_\phi$  of the wave fields) polarization, which propagate in an axial static magnetic field independently of each other. In addition, the Maxwell equations can be solved for these two polarizations separately. The subset of Maxwell equations for each polarization can be written in the form of second order differential equations, e. g., for either  $E_z$  or  $H_z$ , respectively.

On the other hand, studying flute waves also has an obvious disadvantage. They describe specific waves with  $k_z = 0$  only. However, the theory of flute waves can be and has been used as base for studying electromagnetic waves with small axial wavenumbers,  $k_z \neq 0$  [1, 9-11]. In particular, the paper [11] was devoted to the investigation of surface flute waves in circular metal waveguides entirely filled with cold plasma in the presence of an axial static magnetic field. The dispersion properties of surface flute waves in circular metal waveguides partially filled by plasma without any magnetic field were studied in [10]. The initial stage of the interaction of long-wavelength waves of surface type with an annular electron beam gyrating around the plasma column along large Larmor orbits was investigated in [9].

The present study is devoted to investigation of the dispersion properties of surface type waves which propagate with arbitrary azimuthal wave index  $m$  and small axial wavenumber  $k_z$  in circular metal waveguides partially filled with cold collisionless plasma in presence of an axial static magnetic field  $\vec{B}_0$ . Such statement of the problem significantly differs from both considered in [10,11]. The present study generalizes the results in [10] by taking into account an axial static magnetic field, which is applied in many technological devices. At the same time, the investigation carried out in [11] is generalized in the present paper by introducing the

dielectric layer. The latter can, for instance, play an important role in a plasma device preventing interaction between the plasma and the metal wall.

Taking into account the plasma particles' thermal motion is known to result in the appearance of a number of new physical effects. In particular, the propagation of potential surface waves, which do not exist in the Voigt geometry in a cold plasma, becomes possible. Moreover, these “new” waves propagate in different frequency ranges than in the case of cold plasmas. From the mathematical point of view, these new phenomena are the result of including a term proportional to the kinetic pressure gradient into the quasi-hydrodynamic equations of motion for the plasma particles. In other words, the account for the plasma particle thermal motion modifies the plasma permittivity tensor by introducing terms proportional to the Larmor radius squared. This causes the increase of the order of the differential equation which describes the spatial distribution of the wave field with the consequences similar to mode coupling described in the present paper. The properties of the surface waves at the plasma-metal interface, which arise when a hot plasma permittivity tensor is taken into account in the Voigt geometry, were presented in particular in [12,13].

The paper is arranged as follows. The motivation of the study is provided in the present Section I. The model of the plasma-dielectric-metal structure under the consideration, and basic assumptions are described in Section II. The spatial distribution of the wave fields is given in Section III and the dispersion relation is derived in Section IV. Then, the numerical analysis of the dispersion relation is given in Section V. Finally, the obtained results are discussed in the Conclusions, Section VI.

## II. Statement of the problem

The following plasma waveguide structure is under consideration (see Fig. 1). A circular metal waveguide with inner radius  $b$  and infinite electrical conductivity is assumed to be infinite in axial direction  $z$ . The plasma cylinder with radius  $a$  is placed concentrically inside the waveguide. The plasma column is separated from the metal

wall by a dielectric layer with dielectric constant  $\epsilon_d$ . A static magnetic field is directed along the waveguide axis,  $\vec{B}_0 \parallel \vec{z}$ .

The electrodynamic properties of the plasma column are described in terms of the cold collisionless plasma dielectric permittivity tensor  $\epsilon_{ij}$ :

$$\hat{\epsilon} = \begin{pmatrix} \epsilon_1 & i\epsilon_2 & 0 \\ -i\epsilon_2 & \epsilon_1 & 0 \\ 0 & 0 & \epsilon_3 \end{pmatrix}. \quad (1)$$

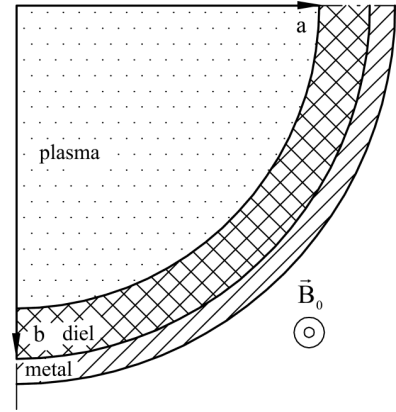


Fig. 1. Schematic of the waveguide geometry

The components of the tensor are given by:

$$\epsilon_1 = 1 - \sum_{\alpha} \frac{\Omega_{\alpha}^2}{\omega^2 - \omega_{\alpha}^2}, \quad \epsilon_2 = - \sum_{\alpha} \frac{\Omega_{\alpha}^2 \omega_{\alpha}}{\omega(\omega^2 - \omega_{\alpha}^2)}, \quad \epsilon_3 = 1 - \sum_{\alpha} \frac{\Omega_{\alpha}^2}{\omega^2}. \quad (2)$$

In (2),  $\Omega_{\alpha}$  is the plasma frequency of the particle of species  $\alpha$  ( $\alpha = i$  for ions and  $\alpha = e$  for electrons), and  $\omega_{\alpha}$  is the corresponding cyclotron frequency.

The present paper employs the method of variable separation. Specifically, one can search for the solution of the Maxwell equations in the following form:

$$H_z(\vec{r}, t) = H_z(r) \exp[i(k_z z + m\phi - i\omega t)]. \quad (3)$$

In (3),  $k_z$ ,  $m$ , and  $\omega$  are the axial wavenumber, azimuthal wave index, and angular wave eigenfrequency, respectively. In this approach, the Maxwell equations can be written in the form of two coupled differential equations of the second order [10,11]:

$$\frac{1}{r} \frac{d}{dr} \left( r \frac{dH_z}{dk_{\perp}^2} \frac{dr}{dr} \right) - H_z \left[ 1 + \frac{m^2}{r^2 k_{\perp}^2} - \frac{m}{r} \frac{d}{dr} \left( \frac{\mu}{k_{\perp}^2} \right) \right] = \hat{R} E_z, \quad (4)$$

$$\frac{1}{k^2 r} \frac{d}{dr} \left( r \frac{dE_z}{dr} \right) + E_z \left[ \frac{\epsilon_3}{1 - k_z^2/k_{\perp}^2} - N_z^2 \right] = \hat{M} H_z. \quad (5)$$

In (4), and (5),  $k_{\perp}^2 = k^2 N_{\perp}^2$ ,  $N_{\perp}^2 = (\epsilon_1 - N_z^2)(\mu^2 - 1) > 0$ , and  $\mu = \frac{\epsilon_2}{(\epsilon_1 - N_z^2)}$ ,  $k = \omega/c$ ,  $N_z = k_z/k$ ,  $N_{\phi} = m/(rk)$ . The right hand sides of eqs. (4) and (5) are small values proportional to the first order of  $k_z$ :

$$\widehat{K}E_z = \frac{iN_z N_\varphi E_z}{k} \frac{d}{dr} \left( \frac{1}{N_z^2} \right) + iN_z \frac{dE_z}{dr} \frac{d}{dr} \left( \frac{\mu}{k_z^2} \right) - \frac{iN_z \mu \varepsilon_3 E_z}{N_z^2}, \quad (6)$$

$$\widehat{M}H_z = \frac{1}{1-k_z^2/k_\perp^2} \left\{ \frac{iN_z}{k_\perp^2} \frac{dH_z}{dr} \frac{d\mu}{dr} + iN_z H_z \left[ \mu - \frac{\mu m}{r} \frac{d}{dr} \left( \frac{\mu}{k_\perp^2} \right) + \frac{m}{r} \frac{d}{dr} \left( \frac{1}{k_\perp^2} \right) \right] \right\}. \quad (7)$$

The presence of a few terms proportional to  $k_z^2$  in the left hand sides of eqs. (4) and (5) provides turning of these equations into those known for the case of wave propagation in a dielectric and/or plasma without any external static magnetic field.

### III. Spatial distribution of the wave fields

In the dielectric region, the wave field distribution is well-known precisely:

$$H_z(r) = G[J'_m(\kappa b)N_m(\kappa r) - N'_m(\kappa b)J_m(\kappa r)], \quad (8)$$

$$E_\varphi(r) = \frac{ik}{-\kappa} G[J'_m(\kappa b)N'_m(\kappa r) - N'_m(\kappa b)J'_m(\kappa r)] - \frac{k_z m}{r \kappa^2} F[J_m(\kappa b)N_m(\kappa r) - N_m(\kappa b)J_m(\kappa r)], \quad (9)$$

$$E_z(r) = F[J_m(\kappa b)N_m(\kappa r) - N_m(\kappa b)J_m(\kappa r)]. \quad (10)$$

In eqs. (8)-(10),  $\kappa^2 = k^2 \varepsilon_d - k_z^2 > 0$ . The expressions (8) and (10) for the amplitudes of the axial electric and magnetic wave fields contain only two constants of integration  $G$  and  $F$  since two other constants are determined from the boundary conditions: the tangential electric wave fields  $E_\varphi$  and  $E_z$  are equal to zero at the metal wall,  $r = b$ .

Within the plasma column, the radial distribution of the wave fields is found by the method of successive approximations. The wave field amplitudes are presented in the form:

$$H_z(r) = H_z^{(0)}(r) + H_z^{(1)}(r), \quad |H_z^{(1)}(r)| \sim |k_z H_z^{(0)}(r)| \ll |H_z^{(0)}(r)|, \quad (11)$$

$$E_z(r) = E_z^{(0)}(r) + E_z^{(1)}(r), \quad |E_z^{(1)}(r)| \sim |k_z E_z^{(0)}(r)| \ll |E_z^{(0)}(r)|. \quad (12)$$

The wave field amplitudes  $H_z^{(0)}(r)$  and  $E_z^{(0)}(r)$ , are assumed to be known from zero approximation, in which  $k_z = 0$ . In other words,  $H_z^{(0)}(r)$  and  $E_z^{(0)}(r)$  are the solutions of eqs. (4) and (5) with zero right hand sides:

$$H_z^{(0)}(r) = A_1 \phi(r) + A_2 \tilde{\phi}(r), \quad (13)$$

$$E_z^{(0)}(r) = C_1 \psi(r) + C_2 \tilde{\psi}(r). \quad (14)$$

In (13) and (14),  $A_{1,2}$  and  $C_{1,2}$  are the constants of integration, the functions  $\phi(r)$  and  $\psi(r)$  are the solutions of eqs. (4) and (5), respectively, with zero right hand sides, which are finite at the axis,  $r = 0$ .

The functions  $\tilde{\phi}(r)$  and  $\tilde{\psi}(r)$  are the solutions of the same equations which are linearly independent from the functions  $\phi(r)$  and  $\psi(r)$ ; they are singular at the axis,  $r = 0$ . The singularity makes it possible immediately to determine two constants of integration,  $A_2 = 0$  and  $C_2 = 0$ .

To find the first order corrections  $H_z^{(1)}(r)$  and  $E_z^{(1)}(r)$  to the radial distributions of the wave fields one can substitute the wave field amplitudes  $H_z^{(0)}(r)$  and  $E_z^{(0)}(r)$  into the right-hand sides of eqs. (4) and (5) instead of full expressions without any loss in precision. Then the corrections  $H_z^{(1)}(r)$  and  $E_z^{(1)}(r)$  are derived by the method of constant variation:

$$H_z^{(1)}(r) = \tilde{\phi} \int_0^r \frac{k_1^2 \phi \tilde{R} E_z^{(0)} dr}{W(\phi, \tilde{\phi})} - \phi \int_a^r \frac{k_1^2 \tilde{\phi} \tilde{R} E_z^{(0)} dr}{W(\phi, \tilde{\phi})}, \quad (15)$$

$$E_z^{(1)}(r) = \tilde{\psi} \int_0^r \frac{k^2 \psi \tilde{M} H_z^{(0)} dr}{W(\psi, \tilde{\psi})} - \psi \int_a^r \frac{k^2 \tilde{\psi} \tilde{M} H_z^{(0)} dr}{W(\psi, \tilde{\psi})}. \quad (16)$$

In (15) and (16),  $W(\phi, \tilde{\phi})$  and  $W(\psi, \tilde{\psi})$  are the Wronskians of the two pairs of functions,

$$W(\phi, \tilde{\phi}) = \phi \frac{\partial \tilde{\phi}}{\partial r} - \tilde{\phi} \frac{\partial \phi}{\partial r}, \quad W(\psi, \tilde{\psi}) = \psi \frac{\partial \tilde{\psi}}{\partial r} - \tilde{\psi} \frac{\partial \psi}{\partial r}. \quad (17)$$

#### IV. Dispersion relation

The calculations presented above describe the radial distribution of the wave field which is sufficient for studying the dispersion properties of electromagnetic waves with arbitrary azimuthal wave indices and small axial wavenumbers in circular metal waveguides with inhomogeneous radial profile of the plasma particle density. However, in the following numerical calculations, a plasma column with uniform

plasma particle density profile is considered to investigate the effect of the non-zero axial wavenumber rather than that of plasma density non-uniformity.

The waves under study should be of surface type. This means that the plasma is nontransparent for these waves. The waves do not propagate in absence of the plasma-dielectric interface in infinite plasma media. A sufficiently dense plasma is considered, so that  $\Omega_e^2 \gg \omega_e^2$ . In this case, surface type waves propagate in the following frequency ranges:

$$|\omega_e| \sqrt{\frac{\Omega_e^2 + c^2 k_z^2}{\Omega_e^2 + \omega_e^2}} < \omega < |\omega_e|, |\omega_e| < \omega < \omega_-. \quad (18)$$

The range (18) encloses the electron cyclotron frequency and is referred hereinafter as low frequency (LF) one. One more range lies above the upper hybrid frequency and is called here as high frequency (HF) one:

$$\sqrt{\omega_e^2 + \Omega_e^2 + c^2 k_z^2} < \omega < \omega_+. \quad (19)$$

In (18) and (19),  $\omega_{\mp}$  are the cut-off frequencies for bulk modes:

$$\omega_{\mp} = \mp 0.5|\omega_e| + \sqrt{0.25\omega_e^2 + \Omega_e^2 + c^2 k_z^2 \frac{\sqrt{0.25\omega_e^2 + \Omega_e^2} \pm 0.5|\omega_e|}{2\sqrt{0.25\omega_e^2 + \Omega_e^2}(\sqrt{0.25\omega_e^2 + \Omega_e^2} \mp 0.5|\omega_e|)}}. \quad (20)$$

Dissipativeless boundary conditions at the plasma-dielectric interface are applied to the solutions derived above for these two regions (plasma column and dielectric layer). The dispersion relation is obtained in the form of a 4x4 determinant,  $|a_{ij}| = 0$ . In this respect the present problem is much more complicated than those solved earlier in [10, 11]. The components of the determinant are listed in Annex 1.

Electron beam excitation of long-wavelength surface waves in the HF range was demonstrated in [9] to be much less efficient as compared with the LF range. That is why the following consideration is restricted to the LF range, though the derived dispersion relation is applicable for studying the dispersion properties of the waves in HF range (19) as well.

## V. Results of the numerical analysis

The dispersion relation is solved numerically. The shape of the dispersion curves are similar to those obtained earlier in [10, 11]. The dependencies of the wave dispersion properties on  $k_z$ ,  $B_0$ , magnitude and sign of  $m$ ,  $\varepsilon_d$ ,  $a$  and  $b$  are studied. The dispersion curves are presented in the form of dependencies of normalized eigenfrequencies  $\omega/|\omega_e|$  on  $k_z a$ .

The results of the numerical studies are presented in Figs. 2-6. As already mentioned, the product  $k_z a$  is chosen as abscissa axis. The present consideration is only valid for small magnitudes of the axial wavenumber. It was analytically derived in [10,11] that the method of successive approximations is applicable in this case of  $k_z \ll m/a$ . The latter condition is fulfilled for all the calculations presented in Figs. 2-6.

The wave eigenfrequency normalized by the electron cyclotron frequency,  $\omega/|\omega_e|$  is chosen as ordinate axis in Figs. 2-5. Since Fig. 6 demonstrates the influence of the external axial static magnetic field on the wave dispersion properties, there the eigenfrequency is normalized by the Langmuir (electron plasma) frequency,  $\omega/\Omega_e$ .

In the case of surface flute waves, the ratio  $m/a$  is the appropriate observable to play the role of the wavenumber and it seems to be natural to normalize this wavenumber by the skin-depth  $\delta = c/\Omega_e$ . Then the effective wavenumber is  $k_{ef} \equiv |m|\delta/a$ , which in Figs. 2-6 is chosen as  $k_{ef} = 0.6$  to make it possible to compare the present results with those reported earlier in [10].

Since ordinary and extraordinary waves are coupled in the present problem, one can see two branches of the dispersion curve in the figures. This is the main distinguishing feature which differs the dispersion properties of surface waves with non-zero axial wavenumber from those of surface flute waves [1].

The branch which turns to surface flute waves in the limit  $k_z \rightarrow 0$  (it almost looks like a horizontal line) is the high frequency (HF) branch. The other branch is characterized by smaller magnitudes of the wave eigenfrequencies (the frequencies



are approximately proportional to  $k_z$ ). That is why this branch is referred here as low frequency (LF) one.

In general, the shapes of all the dispersion curves are similar. For example, in the curve marked by “3” in Fig. 2, the HF branch starts with  $\omega/|\omega_e|=1.903$  for  $k_z=0$ . For small  $k_z < 0.8/a$  the normalized wave eigenfrequency increases to  $\omega/|\omega_e|=1.939$  approximately proportionally to  $k_z^2$ . This circumstance is predictable from the mathematical point of view.

The dispersion relation derived in the present paper can be presented in the following form which is common for the problems of coupled waves:

$$D_X D_O + D^{(2)} = 0. \quad (21)$$

In (21),  $D_X = 0$  is the dispersion relation of extraordinary surface flute waves [1], and  $D_O = 0$  is the dispersion relation of electromagnetic waves with ordinary polarization, the term  $D^{(2)}$  is of the second order of smallness in the axial wavenumber. The solution of the eq. (21) can be presented as a series in  $k_z$ :  $\omega = \omega^{(0)} + \Delta\omega$ , where  $\omega^{(0)}$  is the solution of the dispersion relation in zeroth approximation,  $D_X(\omega^{(0)}) = 0$ . Then the correction  $\Delta\omega$  to the eigenfrequency is given by:

$$\Delta\omega = -\frac{D^{(2)}}{D_O} \left( \frac{\partial D_X}{\partial \omega} \right)_{\omega=\omega^{(0)}} \propto k_z^2. \quad (22)$$

For larger magnitudes of the axial wavenumber,  $0.8/a < k_z < 1.1138/a$ , the HF branch decreases to  $\omega/|\omega_e|=1.766$  to meet with the LF branch. The LF branch decreases almost linearly with decreasing axial wavenumber approaching to the frequency range lower limit (19). For the maximum magnitude of  $k_z = 1.1138/a$ ,

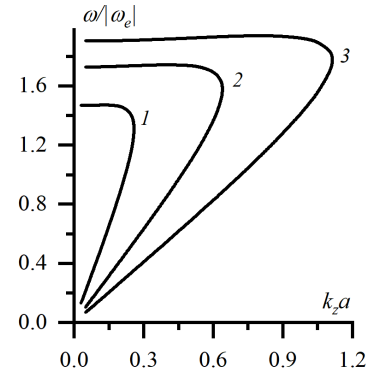


Fig. 2. Surface wave eigenfrequency vs axial wavenumber for different positive azimuthal wave indices  $m=1, 2, 3$  (indicated by the numbers near the curves).  $\epsilon_d = 2, \Delta = (b - a)/a = 0.1, k_{ef} = 0.6, Z = \Omega_e/|\omega_e| = 7.5$

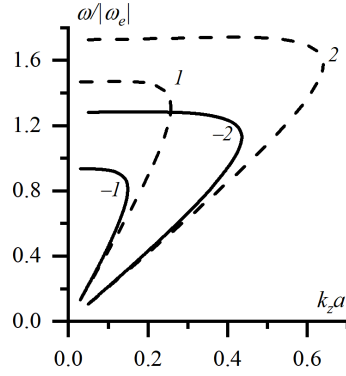


Fig. 3. Surface wave eigenfrequency vs axial wavenumber for azimuthal wave indices of different signs  $m=\pm 1, \pm 2$  (indicated by numbers near the curves).  $\epsilon_d = 2, \Delta = 0.1, k_{ef} = 0.6, Z = 7.5$ . Dashed curves correspond to positive indices, solid curves correspond to the negative indices

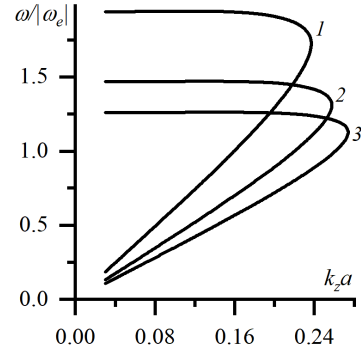


Fig. 4. Surface wave eigenfrequency vs axial wavenumber for different magnitudes of dielectric constant  $\epsilon_d = 1, 2, 3$  (indicated by numbers near the curves).  $m = 1, \Delta = 0.1, k_{ef} = 0.6, Z = 7.5$

the wave group velocity turns to infinity,  $\partial\omega/\partial k_z \rightarrow \infty$ . In the vicinity of this point, the modal representation of the wave fails.

The axial wavenumber for which the frequencies of the HF and LF branches coincide is denoted as  $k_z = k_m$ . Nearby  $k_m$  the representation of electromagnetic eigenwaves in the harmonic form,  $\propto \exp[i(k_z z + m\varphi - \omega t)]$ , fails. Near the point in question, the dispersion curve  $k_z(\omega)$  can be approximately described by the quadratic parabola  $k_z(\omega) = k_m - (\omega - \omega_m)^2/\alpha$  (where  $\alpha$  is a constant having the dimension of acceleration,  $\text{cm/s}^2$ ). In this case, an electromagnetic pulse with the field proportional to  $\exp(-t^2/(2\tau^2))\cos[k_m z + m\varphi - \omega_m t]$  (where  $\tau$  is the pulse duration) spreads out from the point at which it was originally formed in the axial direction over a distance of about  $\alpha\tau^2/2$  [11].

Increasing azimuthal wave index  $m$  is demonstrated in Fig. 2 to cause an increase of the HF branch, which is in agreement with the theory of surface flute waves [1,10,11], and to expansion of the  $k_z$  range where the present consideration is

applicable. The increase of  $m$  from 1 to 3 is accompanied by broadening the  $k_z$  range from  $k_z = 0.257/a$  for  $m=1$  to  $k_z = 0.640/a$  for  $m=2$  and then to  $k_z = 1.114/a$  for  $m=3$  (by 77%).

Figure 3 shows how the sign of the azimuthal wave index influences the wave dispersion properties. The surface flute waves with negative azimuthal wave indices have smaller magnitudes of their eigenfrequencies. That is why the dispersion curves of the waves with  $m < 0$  are shown in Fig. 3 by solid curves which lie lower than those for the waves with positive azimuthal wave indices. The range of axial wavenumbers, where the waves exist, is smaller for the waves with  $m < 0$  than for the waves with positive azimuthal wave indices.

The results presented in Fig. 3 are most appropriate to be compared with those obtained in [10]. In absence of an external static magnetic field  $\vec{B}_0$ , the dispersion properties of electromagnetic waves are known to be degenerate in respect to the sign of the azimuthal wave index  $m$ . Therefore, the influence of the sign of  $m$  on the wave dispersion properties was not studied in [10]. There, the dispersion curve of surface type long-wavelength waves was given for the same plasma waveguide parameters as those applied for the calculations in Fig. 3 of the present paper:  $|m| = 2$ ,  $\varepsilon_d = 2$ ,  $\Delta = 0.1$ ,  $k_{ef} = 0.6$ . However, an external static magnetic field was not considered in [10]. Application of  $\vec{B}_0$  causes the splitting of the dispersion curve. The HF branch of the dispersion curve, which was shown in Fig. 1 of [10], lies in the middle between the HF branches shown in Fig. 3 for  $m = \pm 2$ . The axial wavenumber, for which the frequencies of the HF and LF branches coincide in Fig. 1 of [10], is approximately equal to the arithmetic mean of those for the dispersion curves presented here in Fig. 3 for  $m = \pm 2$ .

The dispersion curves in Fig. 4 demonstrate that the decrease of the HF branch eigenfrequencies does not unambiguously mean narrowing of the  $k_z$  range where the present consideration is applicable. These curves show the effect of the magnitude of the dielectric constant  $\varepsilon_d$  on the wave dispersion properties. Increasing  $\varepsilon_d$  from  $\varepsilon_d = 1$  to  $\varepsilon_d = 2$  and then to  $\varepsilon_d = 3$  results in decreasing maximum magnitude of the

This is the author's peer reviewed, accepted manuscript. However, the online version of record will be different from this version once it has been copyedited and typeset.

PLEASE CITE THIS ARTICLE AS DOI: 10.1063/1.50131261

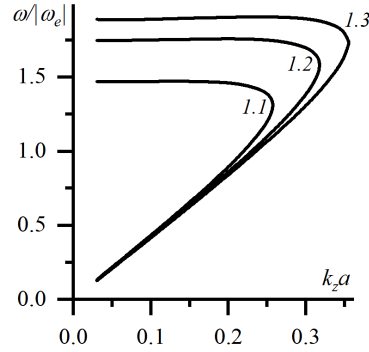


Fig. 5. Surface wave eigenfrequency vs axial wavenumber for different widths of dielectric layer  $b/a = 1.1, 1.2, 1.3$  (indicated by numbers near the curves).  $m = 1, \epsilon_d = 2, k_{ef} = 0.6, Z = 7.5$

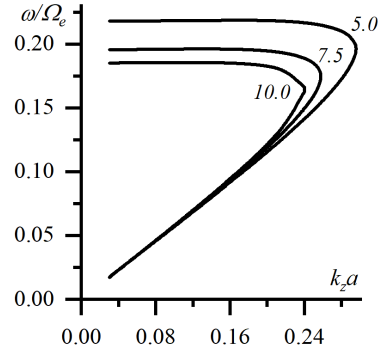


Fig. 6. Surface wave eigenfrequency vs axial wavenumber for different magnitudes of external static axial magnetic field (numbers near the curves indicate the dimensionless parameters  $Z = 5.0, 7.5, 10.0$ ).  $m = 1, b/a = 1.1, \epsilon_d = 2, k_{ef} = 0.6$

HF branch of eigenfrequencies from  $\omega/|\omega_e| = 1.943$  for  $\epsilon_d = 1$  to  $\omega/|\omega_e| = 1.471$  for  $\epsilon_d = 2$  and then to  $\omega/|\omega_e| = 1.262$  for  $\epsilon_d = 3$  (or in other words, by 35% in general), while the maximum of the observed axial wavenumbers increase from  $k_z = 0.237$  for  $\epsilon_d = 1$  to  $k_z = 0.257$  for  $\epsilon_d = 2$  and then to  $k_z = 0.274$  for  $\epsilon_d = 3$  (by 14% only). The decrease of the  $k_z$  range with increasing magnitude of the HF branch eigenfrequencies is pointed out because it is observed in Fig. 4 on the contrary to the tendencies given by Figs. 2, 3, 5 and 6.

The dispersion properties of the waves depend also on the width of the dielectric layer where the waves are of bulk nature (oscillating along the radial coordinate). The wider the layer is, the larger are the eigenfrequencies of the HF branch, and the wider is the  $k_z$  range where the present consideration is applicable (see Fig. 5). Increasing dielectric layer width from  $\Delta = (b - a)/a = 0.1$  to  $\Delta = 0.2$  and then to  $\Delta = 0.3$  (by 67%), causes an increase of the maximum of the wave eigenfrequency of the HF branch from  $\omega/|\omega_e| = 1.471$  for  $\Delta = 0.1$  to  $\omega/|\omega_e| = 1.757$  for  $\Delta = 0.2$  and then to  $\omega/|\omega_e| = 1.905$  for  $\Delta = 0.3$  (by 23%), while the maximum magnitude of the axial

wavenumber increases from  $k_z = 0.257$  for  $\Delta = 0.1$  to  $k_z = 0.318$  for  $\Delta = 0.2$  and then to  $k_z = 0.355$  for  $\Delta = 0.3$  (by 28%).

The results presented in Fig. 5 are most appropriate to be compared with those obtained in [11]. Propagation of long-wavelength electromagnetic waves of surface type in circular metal waveguides entirely filled by cold plasma in presence of an axial static magnetic field was studied there. Surface flute waves are known to be unidirectional in circular metal waveguides entirely filled by cold plasma [1]. In other words, they propagate with azimuthal wave indices of definite sign:  $m > 0$  in the LF range (18) and  $m < 0$  in the HF range (19). Turning the width of the dielectric layer to zero,  $b/a \rightarrow 1$ , makes it impossible for LF surface flute waves with negative  $m$  to propagate. This is one reason more why the dispersion curves shown in Fig. 5 are calculated just for positive azimuthal wave index.

The influence of the magnitude of the external axial static magnetic field  $B_0$  on the dependence of the wave eigenfrequency on the axial wavenumber is shown in Fig. 6. Increasing  $B_0$  is associated with the decrease of the dimensionless parameter  $Z = \Omega_e/|\omega_e|$  which is inversely proportional to  $B_0$ . Doubling of  $Z$  from  $Z = 5.0$  to  $Z = 7.5$  and then to  $Z = 10.0$  causes the decrease of the maximum of the wave eigenfrequency of the HF branch from  $\omega/\Omega_e = 0.219$  for  $Z = 5.0$  to  $\omega/\Omega_e = 0.20$  for  $Z = 7.5$  and then to  $\omega/\Omega_e = 0.186$  for  $Z = 10.0$  (by 15%), while the maximum magnitude of the axial wavenumber decreases from  $k_z = 0.296$  for  $Z = 5.0$  to  $k_z = 0.257$  for  $Z = 7.5$  and then to  $k_z = 0.240$  for  $Z = 10.0$  (by 19%).

The results of the numerical analysis presented in Fig. 2 are applied in the following to demonstrate the wave field radial distribution in Figs. 7 and 8. The following plasma waveguide parameters are chosen for the calculations:  $m = 2$ ,  $\varepsilon_d = 2$ ,  $\Delta = (b - a)/a = 0.1$ ,  $k_{ef} = 0.6$ ,  $Z = \Omega_e/|\omega_e| = 7.5$ . The axial wavenumber is chosen in the middle of the range wherein the surface waves exist as  $k_z a = 0.3$ . In this case surface waves from the LF branch propagate with the frequency  $\omega/|\omega_e| \approx 0.632$ , and those from HF branch – with the frequency  $\omega/|\omega_e| \approx 1.738$ . The radial distribution is presented for the axial magnetic and electric wave fields by solid and

This is the author's peer reviewed, accepted manuscript. However, the online version of record will be different from this version once it has been copyedited and typeset.

PLEASE CITE THIS ARTICLE AS DOI: 10.1063/5.0131261

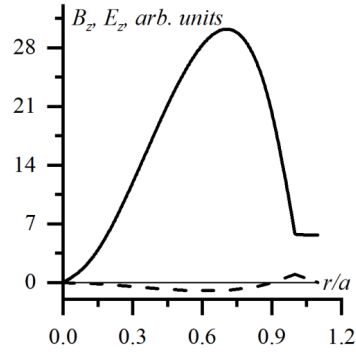


Fig. 7. Radial distribution of the surface wave fields for the LF branch. The solid curve corresponds to the axial magnetic field, and the dashed curve relates to the axial electric field.  $b/a = 1.1$ ,  $m = 2$ ,  $\varepsilon_d = 2$ ,  $k_{ef} = 0.6$ ,  $k_z a = 0.3$ ,  $Z = 7.5$ ,  $\omega/|\omega_e| \approx 0.632$

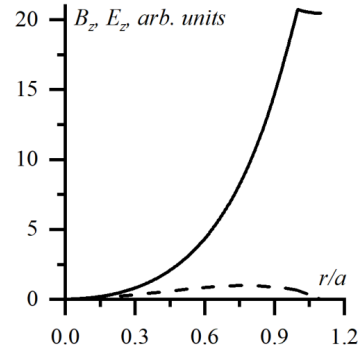


Fig. 8. The same as in Fig. 7, but for the HF branch with  $\omega/|\omega_e| \approx 1.738$

dashed curves, respectively. The field amplitudes are given in arbitrary units. They are normalized in such a way that maxima of the electric field amplitudes are equal to unit. The wave field radial distributions are calculated from eqs. (8), (10), (15), and (16). Both magnetic and electric wave fields turn to zero with approaching to the axis,  $r = 0$ . The electric wave field turns to zero also at the metal wall,  $r = a$ . The magnetic wave field has zero radial derivative at the metal wall.

## VI. Conclusions

The transition from surface flute waves to long-wavelength waves with small magnitude of the axial wavenumber  $k_z$  is accompanied by the appearance of a second branch of the dispersion curve  $\omega = \omega(k_z)$ . This happens due to weak coupling between waves of ordinary and extraordinary polarizations.

The following conclusions can be made from analyzing the influence of different physical observables on the wave dispersion properties. It is the azimuthal wave

This is the author's peer reviewed, accepted manuscript. However, the online version of record will be different from this version once it has been copyedited and typeset.

PLEASE CITE THIS ARTICLE AS DOI: 10.1063/5.0131261

index  $m$  which causes the most influence on the width of the  $k_z$  range where the waves propagate. The influence of the magnitude of  $m$  is much more pronounced than those of the width (which is characterized by the dimensionless parameter  $\Delta$ ) of the dielectric layer between plasma and waveguide wall, and the magnitude of an external axial static magnetic field  $B_0$ . The weakest affect is caused by the magnitude of the dielectric constant  $\epsilon_d$  of the layer.

To summarize the results concerning the group velocity the following issues should be underlined. First, the wave group velocity of the HF branch is small and changes its sign from positive to negative with increasing axial wavenumber. Second, the transfer from the HF branch to the LF branch is accompanied by an increase of the group velocity going to infinity. In addition, the group velocity changes its sign from negative to positive during this transfer. Third, the group velocity of the LF branch does not depend on  $k_z$ , except of the small range of  $k_z$  near the points of transfer from one branch into the other. Fourth, the group velocity of the LF branch varies with varying azimuthal wave index and dielectric constant, and does not vary with the change in the sign of the azimuthal wave index, the width of the dielectric layer, and the magnitude of the external axial static magnetic field.

There is no mathematical problem to generalize the suggested method of solving the Maxwell equations to the case of bulk waves. In the case of uniform radial profile of the plasma particle density, the bulk waves propagate in another frequency range than for surface waves, and are described by Bessel functions of the first and second kinds rather than by the modified Bessel functions.

The suggested method of successive approximations can also be applied for solving the Maxwell equations for electromagnetic waves with small axial wavenumbers in plasma waveguides with inhomogeneous plasma particle density. In this case, even the numerical solution of the Maxwell equations can be simplified since one needs to solve two uniform differential equations of the second order which are independent rather than the similar coupled equations. Including an inhomogeneity of the plasma particle density modifies the surface wave dispersion

relation. The latter can be written in implicit form incorporating the solutions of the Maxwell equations in zeroth approach which are assumed to be known like it is presented in eqs. (15) and (16).

The present study substantially contributes to the development of the theory of plasma waveguides. It generalizes the results of investigating the dispersion properties of long-wavelength electromagnetic waves of surface type in isotropic metal waveguides partially filled by plasma obtained in [10] by introducing an axial static magnetic field. The latter is often applied in modern plasma technological devices. On the other hand, it generalizes the outcomes of research into the eigenfrequencies and spatial distribution of the long-wavelength electromagnetic wave of surface type in magneto-active metal waveguides entirely filled by plasma presented in [11] by taking into account a dielectric layer between the plasma column and the metal wall. In [11], the dispersion relation had the form of the second order determinant on the contrary to the present case and that studied in [10] when the dispersion relation has the form of a fourth order determinant. Combination of these two elements (presence of both axial static magnetic field and the dielectric layer) not only makes the analytic and numerical calculations more complicated but also brings the theoretical model much closer to real conditions of experimental setups.

The presented results can be of interest in the field of plasma electronics and high-power microwave generation and amplification to analyze the interaction of surface-type electromagnetic waves with annual electron beams gyrating in a static axial magnetic field around the plasma column along large Larmor orbits, e.g. in large orbit gyrotrons with circular waveguide cavity [1-9]. In such so-called higher harmonic LOG gyrotrons the azimuthal index of the transverse electric cavity mode is equal to the harmonic number. It operates very close to its cutoff frequency, so that the present approximation of very small axial wavenumber is perfectly fulfilled. The important advantage of the higher harmonic gyro-interaction is, that the necessary strength of the static axial magnetic field in the cavity is divided by the harmonic



number, which makes the needed, very often super-conducting magnet, much cheaper.

### Annex 1.

The components of the determinant  $a_{ij}$  which form the dispersion relation of the studied waves read:

$$a_{11} = I_m(x_1), a_{14} = a_{33} = 0, \quad (\text{A.1})$$

$$a_{12} = K_m(x_1)\mu N_z x_2^2 Q, \quad (\text{A.2})$$

$$a_{13} = J_m(x_3)N'_m(x_4) - J'_m(x_4)N_m(x_3), \quad (\text{A.3})$$

$$a_{21} = \frac{\mu m}{x_1^2} I_m(x_1) + \frac{I'_m(x_1)}{x_1}, \quad (\text{A.4})$$

$$a_{22} = x_2^2 \left(1 - \frac{k_z^2}{k_\perp^2}\right) N_z Q \left(\frac{\mu m}{x_1^2} K_m(x_1) + \frac{K'_m(x_1)}{x_1}\right) + \frac{\mu N_z x_2 I'_m(x_2)}{x_1^2} + \frac{N_z m}{x_1^2} I_m(x_2), \quad (\text{A.5})$$

$$a_{23} = \frac{1}{x_3} [J'_m(x_4)N'_m(x_3) - J'_m(x_3)N'_m(x_4)], \quad (\text{A.6})$$

$$a_{24} = \frac{N_z m}{x_3^2} a_{34}, \quad (\text{A.7})$$

$$a_{31} = K_m(x_2)k_z k a^2 \mu Q / (1 - k_z^2/k_\perp^2), \quad (\text{A.8})$$

$$a_{32} = -I_m(x_2), \quad (\text{A.9})$$

$$a_{34} = J_m(x_4)N_m(x_3) - J_m(x_3)N_m(x_4), \quad (\text{A.10})$$

$$a_{41} = \frac{k_z \mu}{k_\perp} I'_m(x_1) + \frac{k_z m}{k_\perp^2 a} I_m(x_1) + \frac{K'_m(x_2)x_2 k_z a \mu Q}{1 - k_z^2/k_\perp^2}, \quad (\text{A.11})$$

$$a_{42} = -\frac{x_2}{ka} I'_m(x_2), \quad (\text{A.12})$$

$$a_{43} = -\frac{mk_z a}{x_3^2} a_{13}, \quad (\text{A.13})$$

$$a_{44} = \frac{\kappa}{k} [J_m(x_4)N'_m(x_3) - J'_m(x_3)N_m(x_4)], \quad (\text{A.14})$$

$$Q = \frac{a^2}{x_1^2 - x_2^2} [x_1 I_m(x_2)I_{m+1}(x_1) - x_2 I_m(x_1)I_{m+1}(x_2)], \quad (\text{A.15})$$

$$x_1 = k_\perp a, x_2 = ak \sqrt{-\frac{\epsilon_3}{1 - k_z^2/k_\perp^2}}, x_3 = \kappa a, x_4 = \kappa b. \quad (\text{A.16})$$

### Acknowledgements

This work is partially supported by the Ministry of Education and Science of Ukraine Research Grant 0119U002526.

### Data Availability

The data that supports the findings of this study are available within the article.

### References

1. I. Girka, and M. Thumm, *Surface flute waves in plasmas. Eigenwaves, excitation, and applications* (Springer, Cham, 2022).
2. W. Lawson, and C. D. Striffler, "A general linear growth rate formula for large orbit, annular electron beams," *Physics of Fluids*, **28**, No. 9, 2868-2977 (1985).
3. W. W. Destler, E. Chojnacki, R. F. Hoeberling, W. Lawson, A. Singh, and C. D. Striffler, "High-power microwave generation from large-orbit devices," *IEEE Transactions on Plasma Science*, **16**, No. 2, 71-89 (1988).
4. V. D. Yermka, V. A. Zhurakhovsky, and V. P. Shestopalov, "Large-orbit peniotron profiled from the law of through gyroresonance," *Radiotekhnika I Elektronika*, **34**, No. 9, 1900-1907 (1989). (in Russian).
5. V. L. Bratman, Yu. K. Kalynov, V. N. Manuilov, and S. V. Samsonov, "Large orbit gyrotron at submillimeter waves," *Conf. Digest 30th Int. Conf. on Infrared and Millimeter Waves and 13th Int. Conf. on Terahertz Electronics*, Williamsburg, VA, USA, 443-444 (2005).
6. V. L. Bratman, Yu. K. Kalynov, V. N., Manuilov, and S. V. Samsonov, "Large-orbit gyrotron operation at submillimeter waves," In: *Proc. 6th Int. Workshop on Strong Microwaves in Plasmas*, Nizhny Novgorod, ed. A.G. Litvak, Institute of Applied Physics, Russian Academy of Sciences, Nizhny Novgorod, 2006, **1**, 150-155 (2005).
7. F. Li, W. He, A. W. Cross, C. R. Donaldson, L. Zhang, A. D. R. Phelps, and K. Ronald, "Design and simulation of a  $\sim 390$  GHz seventh harmonic gyrotron using a large orbit electron beam," *J. Phys. D Appl. Phys.*, **43**, 155204 (2010).
8. X. Li, J. Lang, Y. Alfadhil, and X. Chen, "Study of an eighth-harmonic large-orbit gyrotron in the terahertz band," *IEEE Transactions on Plasma Science*, **43**, 506-514 (2015).
9. I. O. Girka, O. I. Girka, and M. Thumm, "Initial stage of interaction between gyrating relativistic electron beam and long wavelength surface electromagnetic waves in cylindrical metallic wave-guides partially filled with plasma," *Physics of Plasmas*, **26**, No. 4, 042118 (2019).
10. V. A. Girka, and I. A. Girka, "Asymmetric long-wavelength surface modes of isotropic plasma waveguides," *Plasma Physics Reports*, **28**, No. 8, 682-689 (2002).

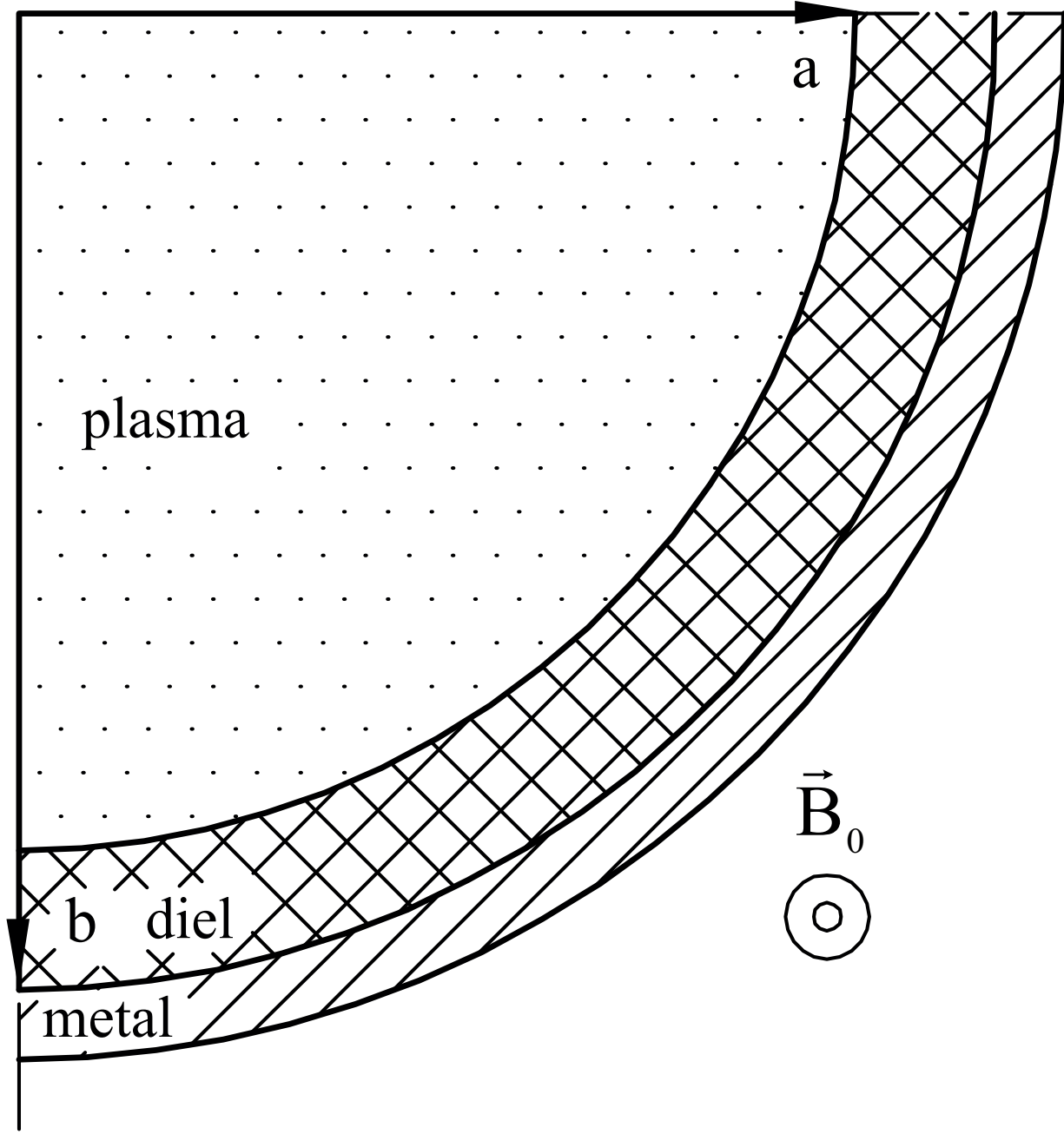
This is the author's peer reviewed, accepted manuscript. However, the online version of record will be different from this version once it has been copyedited and typeset.

PLEASE CITE THIS ARTICLE AS DOI: 10.1063/5.0131261

11. V. O. Girka, and I. O. Girka, "Asymmetric long-wavelength surface waves in magnetized plasma waveguides entirely filled with plasma," *Plasma Physics Reports*, **28**, No. 11, 916–924 (2002).
12. N. A. Azarenkov, K. N. Ostrikov, "High-frequency potential surface waves at the boundary between a magnetoactive terminal-pressure plasma and a metal," *Plasma Physics Reports*, **17**, No. 3, 316-320 (1991). In Russian.
13. N. A. Azarenkov, K. N. Ostrikov, "Potential surface waves in a warm nonisothermal plasma bounded by metal," *Contributions to Plasma Physics*, **31**, No. 6, 637-646 (1991).

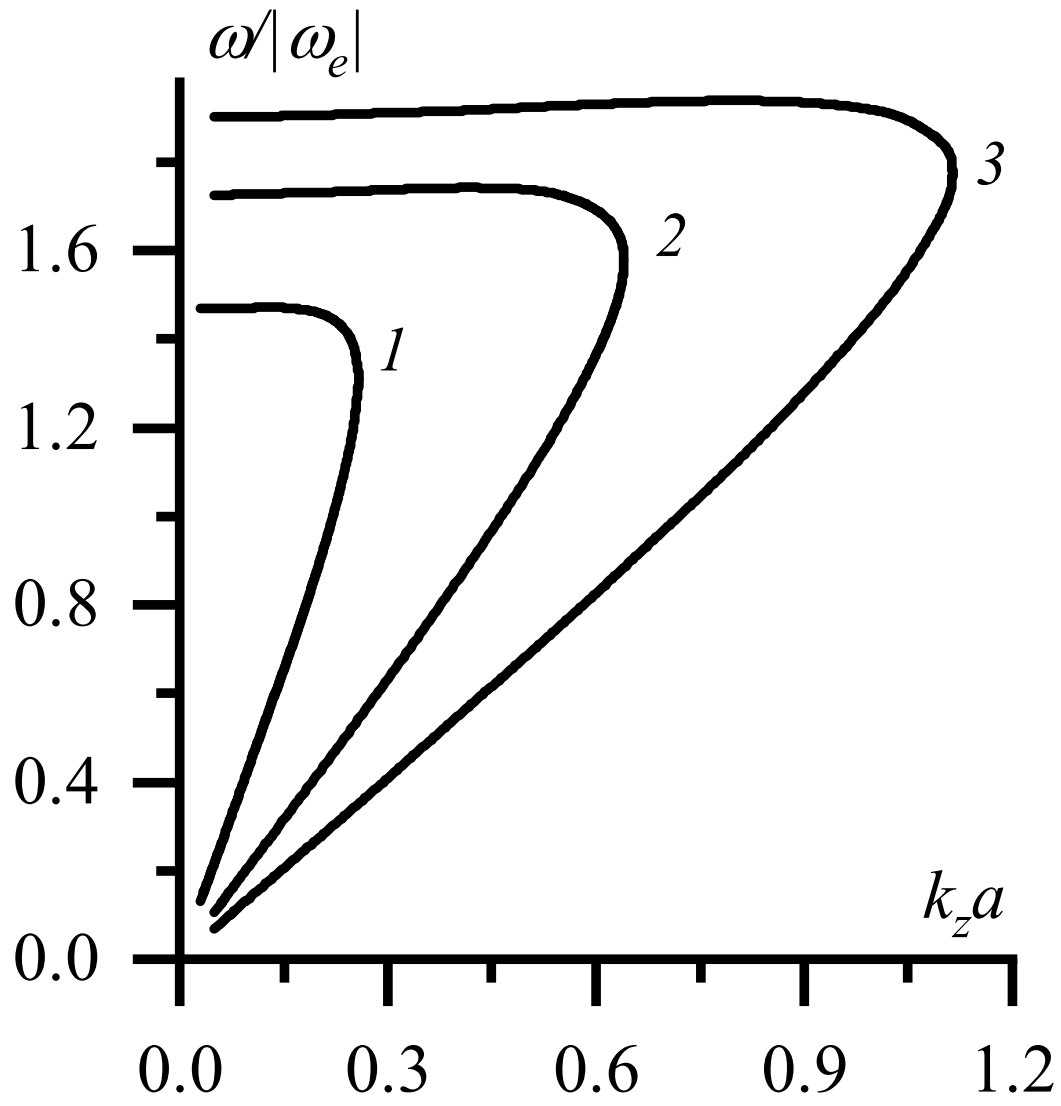
This is the author's peer reviewed, accepted manuscript. However, the online version of record will be different from this version once it has been copyedited and typeset.

PLEASE CITE THIS ARTICLE AS DOI: 10.1063/5.0131261



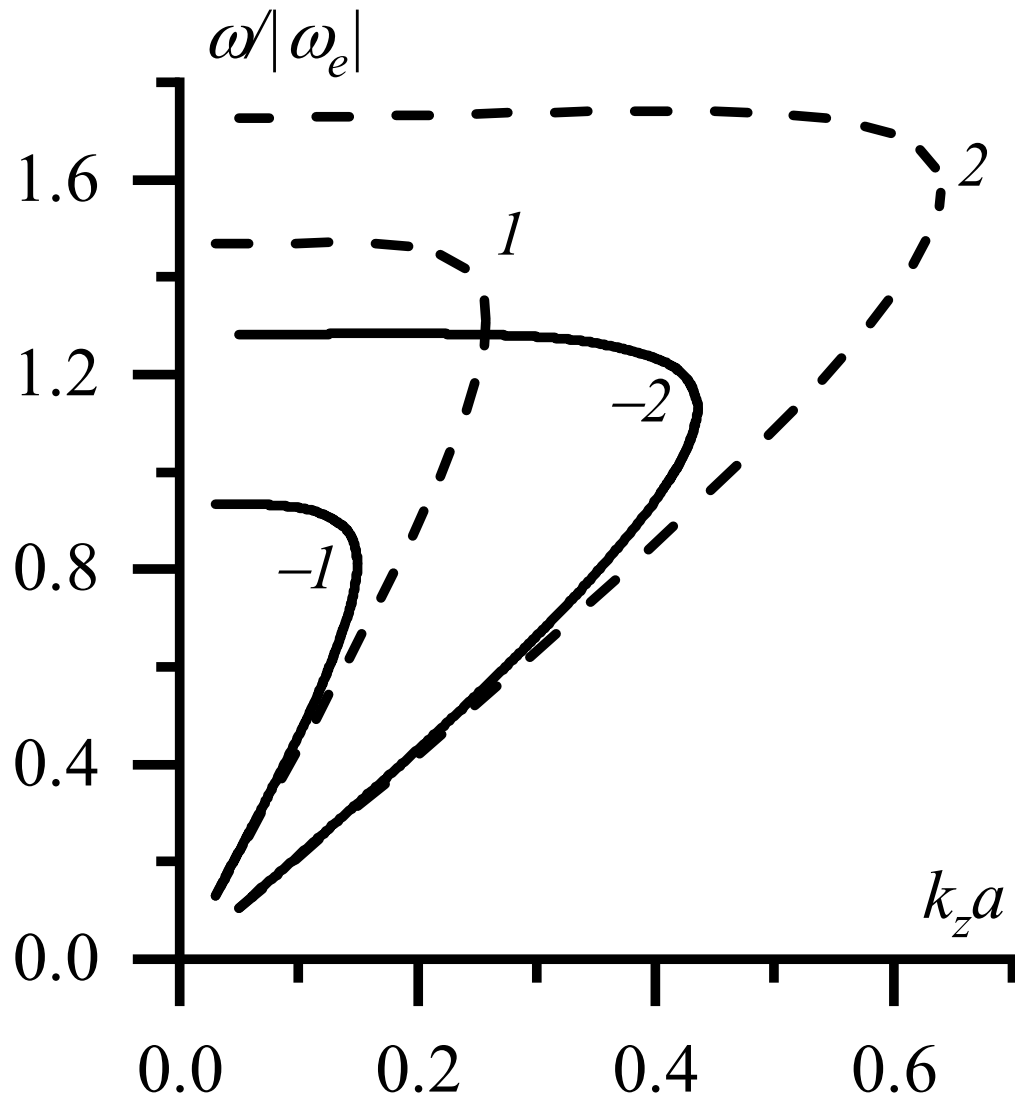
This is the author's peer reviewed, accepted manuscript. However, the online version of record will be different from this version once it has been copyedited and typeset.

PLEASE CITE THIS ARTICLE AS DOI: 10.1063/5.0131261



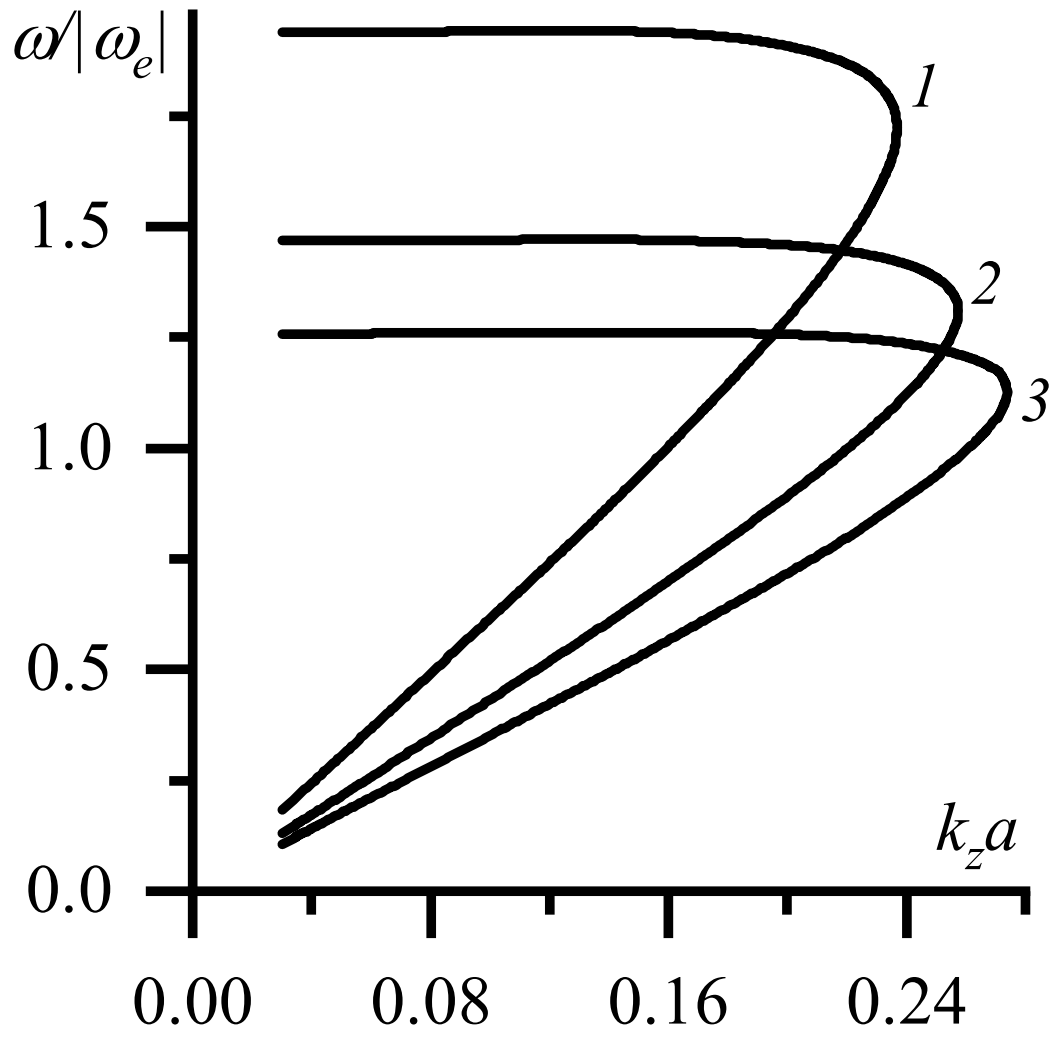
This is the author's peer reviewed, accepted manuscript. However, the online version of record will be different from this version once it has been copyedited and typeset.

PLEASE CITE THIS ARTICLE AS DOI: 10.1063/5.0131261



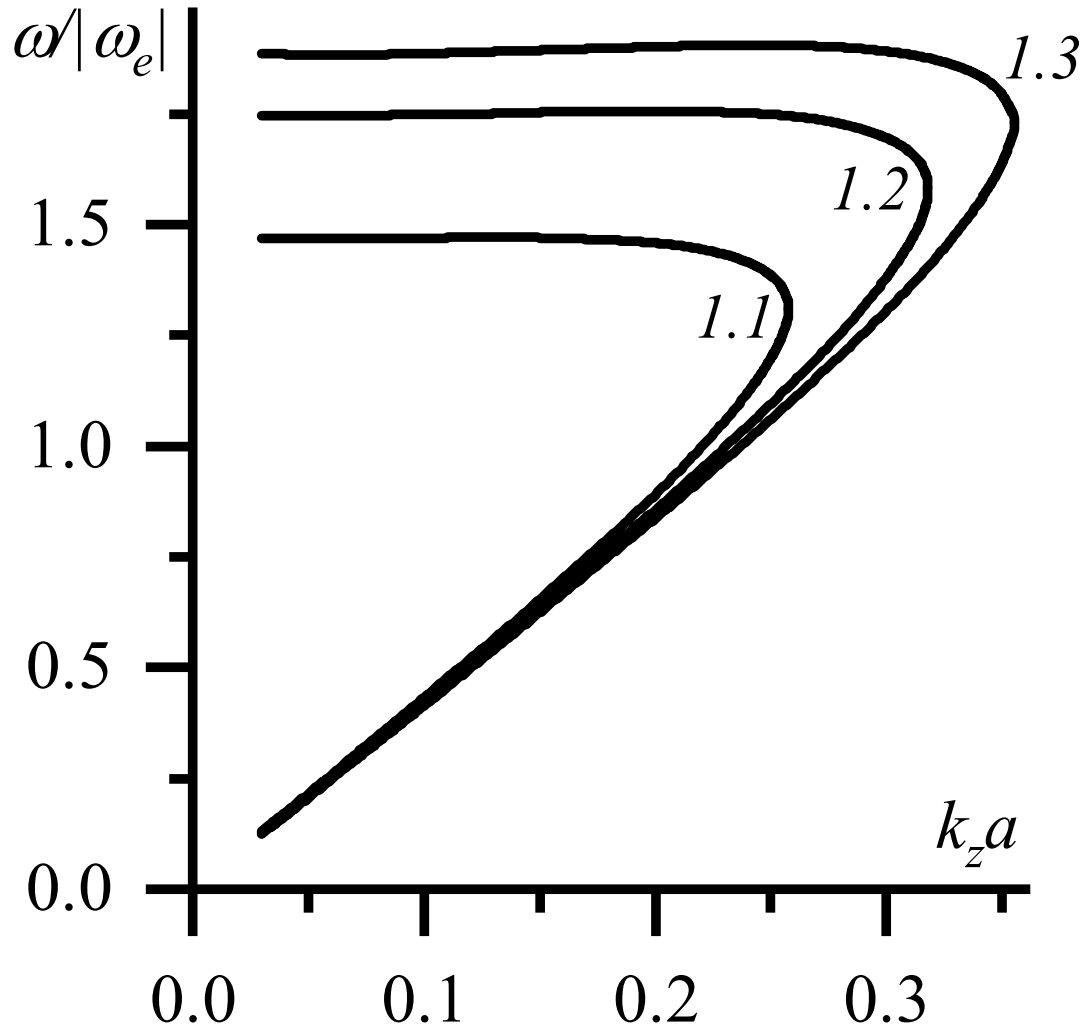
This is the author's peer reviewed, accepted manuscript. However, the online version of record will be different from this version once it has been copyedited and typeset.

PLEASE CITE THIS ARTICLE AS DOI: 10.1063/5.0131261



This is the author's peer reviewed, accepted manuscript. However, the online version of record will be different from this version once it has been copyedited and typeset.

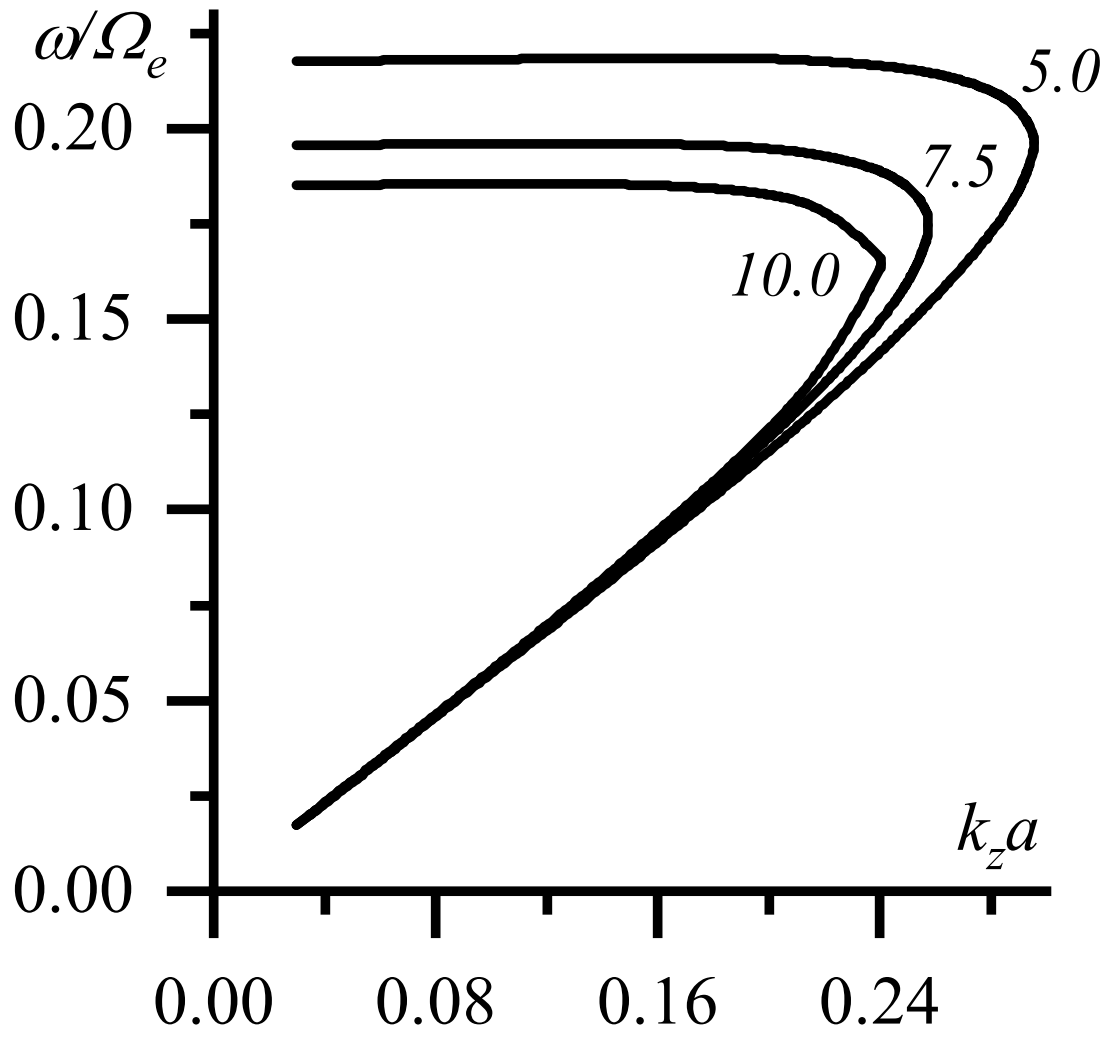
PLEASE CITE THIS ARTICLE AS DOI: 10.1063/5.0131261





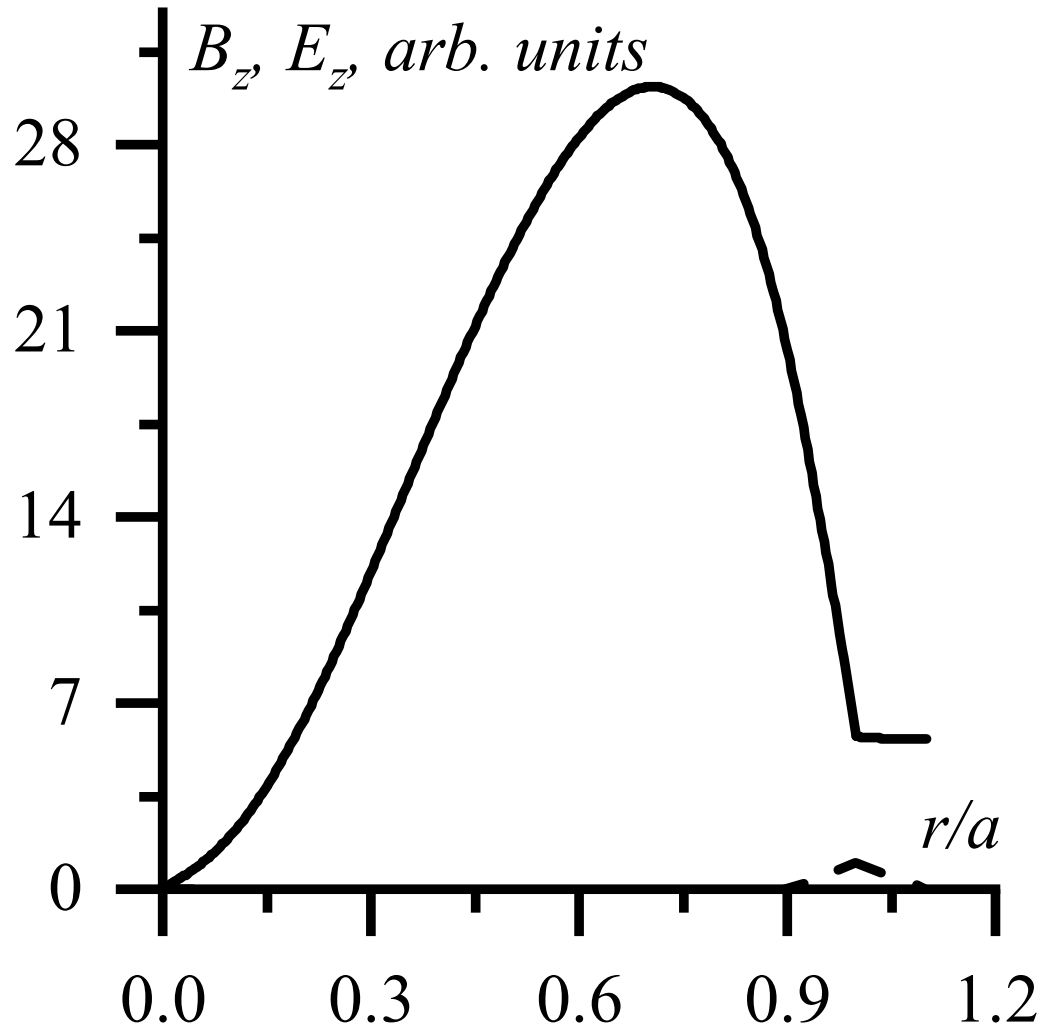
This is the author's peer reviewed, accepted manuscript. However, the online version of record will be different from this version once it has been copyedited and typeset.

PLEASE CITE THIS ARTICLE AS DOI: 10.1063/5.0131261



This is the author's peer reviewed, accepted manuscript. However, the online version of record will be different from this version once it has been copyedited and typeset.

PLEASE CITE THIS ARTICLE AS DOI: 10.1063/5.0131261



This is the author's peer reviewed, accepted manuscript. However, the online version of record will be different from this version once it has been copyedited and typeset.

PLEASE CITE THIS ARTICLE AS DOI: 10.1063/5.0131261

